Proceedings of the 12th International Conference on Quasicrystals (ICQ12)

Tsai-Type Quasicrystal and Its Approximant in Au–Al–Tm Alloys

K. Tanaka[a], Y. Tanaka[a], T. Ishimasa[a,*], M. Nakayama[b], S. Matsukawa[b], K. Deguchi[b] and N.K. Sato[b]

[a]Division of Applied Physics, Graduate School of Engineering, Hokkaido University, Sapporo 060-8628, Japan
[b]Department of Physics, Graduate School of Science, Nagoya University, Nagoya 464-8602, Japan

A P-type icosahedral quasicrystal with a six-dimensional lattice parameter $a_{6D} = 7.411$ Å is formed as an equilibrium phase in Au–Al–Tm alloy, of which composition was analyzed to be $Au_{46}Al_{38}Tm_{16}$ by electron probe microanalysis. This quasicrystal is observed as a predominant phase in both as-cast and $Au_{49}Al_{34}Tm_{17}$ alloys annealed at 910 °C, and as one of main phases in the alloy slowly cooled from 1020 °C. A 1/1 approximant, $Au_{48}Al_{38}Tm_{14}$, is also formed near the composition of the quasicrystal. This is a body-centered cubic structure (space group: $Im\bar{3}$) with a lattice parameter $a = 14.458$ Å that is an isostructure to the recently reported 1/1 Tsai-type approximant in Au–Al–Yb. This approximant is characterized by disorderly arranged four Au–Al atoms centered at the Tsai-type cluster, presence of atoms at 8c site, and chemical ordering of Au and Al at sites forming a partial triacontahedron.

DOI: 10.12693/APhysPolA.126.603
PACS: 61.66.Dk, 61.44.Br

1. Introduction

After the report of the first Tsai-type quasicrystals in Cd–Mg–R (R = rare earth element or Ca) [1], new members of this type have been discovered in Cu, Zn, Pd, Ag, Cd, and Au-based alloys (see for example [2] and references therein). They were discovered by either applying substitution rule satisfied in Tsai-type quasicrystals [3, 4] or modifying corresponding approximants already reported. The substitution rule is composed of two conditions on valence electron concentration e/a and atomic size factor [3, 4]. An approximant is a crystal consisting of periodic arrangement of so-called Tsai-type cluster. Approximants are important as a "standard" to study various aspects of quasicrystals: atomic arrangement, formation condition, and chemical and physical properties. In particular, recent studies on 1/1 cubic approximants have clarified their unique structural characteristics. One is geometrically disordered arrangement of atoms near the central region of each cluster. This is basically orientational disorder of four atoms tetrahedrally arranged. The surrounding shell, namely dodecahedron, is distorted reflecting the orientation of the inside tetrahedron. This type of disorder may be either static [5] or dynamic [6]. The other interesting property is presence of atoms at 8c site located at [1/4 1/4 1/4] in the cubic cell (space group: $Im\bar{3}$). It is known that the occupation of this special site strongly depends on alloy system [7], and in many cases no atom exists at this site. Accordingly, so-called "Tsai-type 1/1 approximant" is not an isostructure in a strict sense, and then careful characterization of each approximant is necessary.

*corresponding author; e-mail: ishimasa@eng.hokudai.ac.jp

In this study we treat the Au–Al–Tm system. Au-based quasicrystals and approximants are rather new, and have been found by applying the above substitution rule; namely Cd atom in Cd–R was substituted by Au–X (X = Al [2], Ga [8], In [9, 10], Ge [11, 12], and Sn [10, 13]). We will report formation of an icosahedral quasicrystal and the corresponding approximant in Au–Al–Tm system.

2. Experimental

Au–Al–Tm alloys were prepared from pure elements of Au (99.99%), Al (99.999%), and Tm (99.9%). Alloy ingots with nominal compositions $Au_xAl_{100-x-y}Tm_y$ were synthesized in the narrow region of $48 < x < 53$ and $15 < y < 20$ referring to the stoichiometry of the $Au_{51}Al_{34}Yb_{15}$ quasicrystal. They were alloyed by arc-melting under an atmosphere of high-purity Ar on a water-cooled Cu hearth. Before further heat treatment, a specimen was sealed in a silica ampoule after evacuation to approximately 10^{-6} Torr. Three types of specimens were made by (1) arc-melting without further heat treatment, (2) arc-melting plus annealing between 800 °C and 910 °C for 50–150 h, (3) arc-melting plus re-melting in a graphite crucible at 1020 °C followed by slow cooling to 820 °C with cooling rate 8.3 K/h. Hereafter these three types will be referred to as as-cast, annealed, and re-melted specimens, respectively.

Powder X-ray diffraction experiments were carried out by a RINT-2000 diffractometer using Cu K_α-radiation. Details of the intensity measurement for the Rietveld refinement was described elsewhere [2]. The refinement was carried out using the software package RIETAN-2000 developed by Izumi and Ikeda [14]. The structure model was drawn using Balls & Sticks software [15]. Electron microscopic observation was carried out using JEOL JEM200CS microscope operating at 200 kV with a dou-

ble tilting stage. The alloy specimen was crushed by an agate mortar and a pestle, and a thin part of the fragment was observed. Compositions of the phases formed in the Au–Al–Tm alloys were analyzed by electron probe microanalyzer (EPMA) at acceleration voltage of 20 kV using JXA-8900M microanalyzer with a wavelength dispersive type spectrometer. Differential thermal analysis (DTA) was carried out in the temperature range between 500 and 1020 °C with heating rate 10 K/min in an atmosphere of pure Ar. In this analysis a powder of Al_2O_3 was used as a standard material.

3. Result and discussion

3.1. Formation conditions of quasicrystal and approximant

A P-type icosahedral quasicrystal was formed as a major phase in the as-cast and annealed specimens of both $Au_{49}Al_{34}Tm_{17}$ and $Au_{48}Al_{35}Tm_{17}$. Powder X-ray diffraction pattern of the $Au_{49}Al_{34}Tm_{17}$ alloy annealed at 910 °C for 70 h is presented in Fig. 1a. The reflections of the icosahedral quasicrystal were indexed as P-type with the six-dimensional lattice parameter a_{6D} = 7.411 (2) Å. The quasicrystal was also observed in the re-melted specimen (Fig. 1b), but was distributed unevenly. In some region we observed few quasicrystals, where two other phases were identified; one is a 1/1 approximant described below, and the other $Mn_{23}Th_6$-type ($D8_a$) with a lattice parameter a = 12.82 (1) Å. Alloy compositions of these phases were analyzed by EPMA; the quasicrystal: $Au_{46}Al_{38}Tm_{16}$, the 1/1 approximant: $Au_{48}Al_{38}Tm_{14}$, and the $Mn_{23}Th_6$-type: $Au_{50}Al_{30}Tm_{20}$.

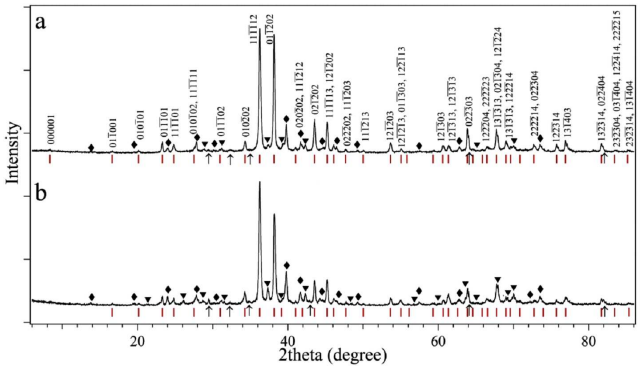

Fig. 1. Powder X-ray diffraction patterns of two $Au_{49}Al_{34}Tm_{17}$ specimens measured by Cu K_α-radiation. (a) Annealed at 910 °C for 70 h and (b) re-melted at 1020 °C for 5 h and slowly cooled to 820 °C with cooling rate 8.3 K/h. Red bars at lower parts indicate diffraction peaks originating from quasicrystal. Major reflections of quasicrystal were indexed by six-dimensional indices. Arrowheads and small rhombuses indicate reflections due to 1/1 approximant and $Mn_{23}Th_6$-type phase, respectively. Remaining unidentified peaks with very weak intensity are indicated by arrows.

Three typical electron diffraction patterns of the icosahedral quasicrystal are presented in Fig. 2, which indicate diffraction symmetry $m\overline{35}$. In the 2-fold diffraction pattern presented in Fig. 2a, one can notice the presence of τ^3-scaling that is indicative of P-type. The structural improvement caused by heat treatment is evident in Fig. 3 that is a series of 3-fold diffraction patterns of three types of specimens. The deviation of a weak reflection from the ideal position observed in the as-cast specimen almost disappeared in the annealed and re-melted specimen. Weaker reflections appear in the re-melted specimen which were not observed in the as-cast specimen. Corresponding to this result, the peak width, full width at half maxima, of $02\overline{2}\overline{3}03$ reflection at $2\theta = 63.9°$ in the powder X-ray diffraction pattern was decreased from $\Delta(2\theta) = 0.34°$ in the as-cast specimen to 0.23° in the annealed and 0.14° in the re-melted ones.

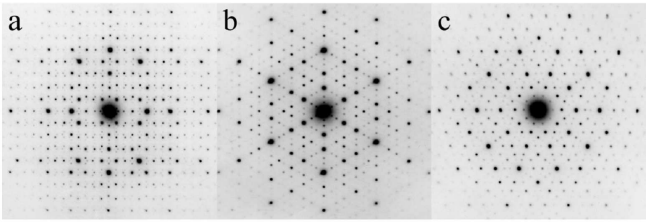

Fig. 2. Selected-area electron diffraction patterns of quasicrystal formed in $Au_{49}Al_{34}Tm_{17}$ alloy annealed at 920 °C for 106 h. Beam incidence along (a) 2-fold, (b) 3-fold and (c) 5-fold axes. Notice τ^3-scaling that can be seen in (a).

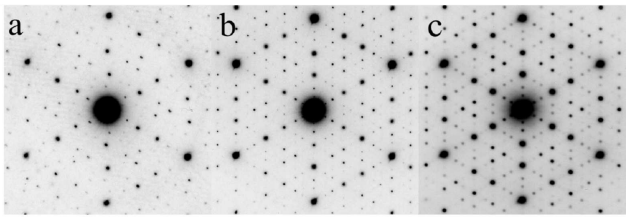

Fig. 3. Magnified electron diffraction patterns with beam incidence along 3-fold axis. (a) Quasicrystal in as-cast $Au_{48}Al_{35}Tm_{17}$ alloy, (b) quasicrystal in $Au_{49}Al_{34}Tm_{17}$ alloy annealed at 920 °C for 106 h and (c) quasicrystal in $Au_{49}Al_{34}Tm_{17}$ alloy re-melted at 1020 °C for 5 h and slowly cooled to 820 °C with cooling rate 8.3 K/h. Notice deviation of diffraction spots from the ideal positions in (a) is reduced in (b) and (c).

In the elevated temperature process, DTA curve, Fig. 4a, of the 1/1 approximant exhibited a single endothermic peak with a maximum at 996 °C. The DTA curve of the $Au_{49}Al_{34}Tm_{17}$ specimen, mainly including the quasicrystal, exhibited three endothermic peaks with maxima at 984, 996, and 1007 °C, the second of which is assigned to the melting of the 1/1 approximant (see Fig. 4b). The peak at 984 °C is assigned to decomposition of the quasicrystal. The small endothermic peak at 1007 °C is interpreted as melting of the $Mn_{23}Th_6$-type phase, and above this temperature complete liquid may appear. Then it is possible to speculate the sequence of the phase formation in the cooling process from the

melt. First the $Mn_{23}Th_6$-type phase is solidified, and then the 1/1 approximant is formed. Finally the quasicrystal is formed probably by peritectic or peritectoid reaction. This complicated formation process may be the reason why 100% specimen of the quasicrystal was not synthesized by the re-melting and slow cooling method, even though the quasicrystal is an equilibrium phase in the Au–Al–Tm system. It is noted that the annealing temperature, 910 °C, applied in this experiment is below the decomposition temperature of the quasicrystal, and no other reaction was detected between these temperatures. This fact is an evidence of the stability of the quasicrystal.

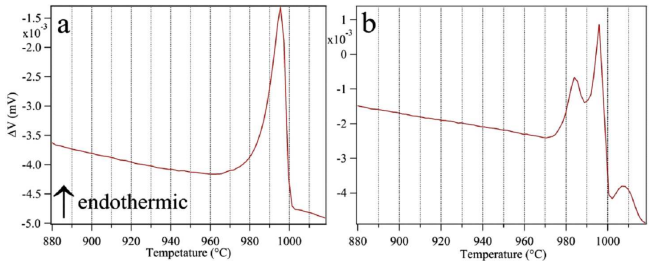

Fig. 4. DTA curves of (a) $Au_{49}Al_{36}Tm_{15}$ alloy re-melted at 1010 °C for 5 h and annealed at 802 °C for 24 h including 1/1 approximant exclusively, and (b) $Au_{49}Al_{34}Tm_{17}$ alloy annealed at 910 °C for 70 h mainly consisting of quasicrystal as presented in Fig. 1a. Notice common endothermic peak at 996 °C in (a) and (b).

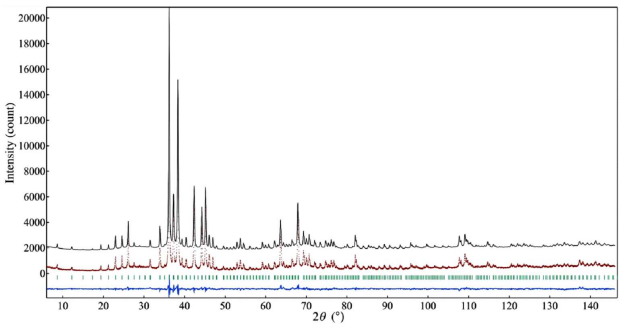

Fig. 5. Powder X-ray diffraction pattern of $Au_{49}Al_{36}Tm_{15}$ annealed at 910 °C for 56 h. Calculated intensity, measured intensity, peak positions of the approximant, and deviation are presented in this order.

The 1/1 approximant was formed exclusively in the specimens with the nominal composition $Au_{49}Al_{36}Tm_{15}$, which were annealed between 800 and 910 °C for 50–100 h. The powder X-ray diffraction pattern and the electron diffraction patterns of the 1/1 approximant are shown in Figs. 5 and 6, respectively. The electron diffraction experiment revealed the Laue class $m\bar{3}$. The cubic lattice is a body-centered type with lattice parameter $a = 14.458$ (1) Å. These observations are in agreement with the known properties of a 1/1 cubic approximant of the Tsai-type. Assuming the relationship between the six-dimensional lattice parameter $a_{6D} = 7.411$ Å and the

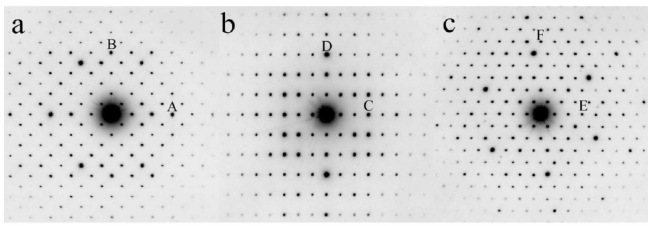

Fig. 6. Selected-area electron diffraction patterns of 1/1 approximant formed in annealed $Au_{49}Al_{36}Tm_{15}$ alloy: (a) [001], (b) [101] and (c) [111]. Reflections indicated by letters are A: 600, B: 060, C: $30\bar{3}$, D: 060, E: $30\bar{3}$, F: $\bar{3}6\bar{3}$.

lattice parameter of 1/1 approximant a, it is possible to calculate expected value $a = 14.425$ Å that agrees well with the measured one.

According to the results of EPMA, the compositions of the quasicrystal and the approximant are $Au_{46}Al_{38}Tm_{16}$ and $Au_{48}Al_{38}Tm_{14}$, respectively. The valence electron concentrations e/a are calculated to be respectively 2.08 and 2.02 by assuming valences of Au: 1, Al: 3, and Tm: 3. They are typical values for Tsai-type quasicrystals and approximants, both of which range between 1.95 to 2.15 [3, 4]. The content of rare-earth element is always slightly higher in quasicrystals than in the corresponding approximants. This is also the case in the Au–Al–Tm quasicrystal and the approximant.

3.2. Crystal structure of 1/1 approximant

The Rietveld analysis of the 1/1 approximant was carried out by assuming the space group $Im\bar{3}$. A structure model of 1/1 Au–Al–Yb approximant was used as starting model. Here Yb atoms in the initial model were replaced by Tm atoms. The ratio between Au and Al in each site was changed stepwise to achieve better fit to the measured intensity distribution. In the final stage of the refinement, we carefully checked the following two points. One is local structure in the central region of the Tsai-type cluster and the other is existence of an atom centered at [1/4 1/4 1/4]. For the former, four possible models were tested, namely partially occupied 12d, 16f, 24g, and 48h. In the result, their R_{wp} were 6.93%, 5.92%, 5.89%, and 5.85% for 12d, 16f, 24g, and 48h, respectively, by assuming 100% presence of [1/4 1/4 1/4] atom. For the latter, the following three models were tested, namely fully or partially occupied 8c site and splitting site of 16f-type centered at [1/4 1/4 1/4] with partial occupancy. While the splitting 16f model has one additional parameter comparing with the 8c model, this did not show decisive advantage against the 8c model. The final model with partially occupied 48h and fully occupied 8c sites exhibited the best fit with $R_{wp} = 5.85\%$, $R_I = 1.12\%$ and $R_F = 0.78\%$. The result of the Rietveld refinement is summarized in Table.

The atomic arrangement of this model is presented in Fig. 7. The unit cell includes 176.0 atoms, namely 87.8 Au, 64.2 Al, and 24.0 Tm. The composition of this model is $Au_{49.9}Al_{36.5}Tm_{13.6}$ that agrees with the composition $Au_{48}Al_{38}Tm_{14}$ analyzed by EPMA as well as

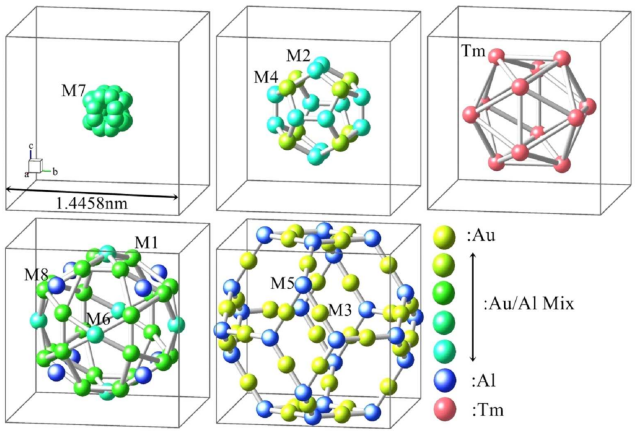

Fig. 7. Structure model of Au–Al–Tm approximant viewed along [0.97 0.17 0.17] direction.

the nominal composition $Au_{49}Al_{36}Tm_{15}$. The structure of the 1/1 approximant can be regarded as a periodic arrangement of Tsai-type clusters with chemical ordering. These cluster are embedded in the cage formed by M3(Au) and M5(Al) sites as shown in Fig. 7. This cage is regarded as a part of triacontahedron with edge-centered atom M3. Such chemical ordering on the triacontahedron shell is the common properties of Au-based 1/1 approximants [2, 8, 11–13]. Other sites are occupied by mixed atoms of Au and Al except for Tm and M8(Al) sites. These structural properties are very similar to those in Au–Al–Yb [2] and Au–Ga–Ca [11] approximants comparing with other 1/1 approximants, and then these three approximants can be regarded as isostructure in a strict sense.

With respect to the B-factors or the atomic displacement parameters $U_{eq} = B/(8\pi^2)$, those at some specific sites are relatively large, namely at M2, M7, and M8 sites. The large value of B of M8 site may be related to the possible occurrence of splitting described above. M7 site corresponding to the inner tetrahedron has partial occupancy 1/6 and large value of B. With respect to this fact, there are two possible interpretations. One is dynamic movement of the tetrahedron recently observed in Zn_6Sc approximant [6], and the other is static and disordered arrangement of tetrahedron [5] that also causes relatively large displacement of M2 and M4 forming the outer dodecahedral shell. For the static model, short-range order of Au and Al may play important role as depicted in Fig. 2 in [5], in which local segregation of Cu and Al atoms on M2 and M4 takes place in the case of Cu–Al–Sc 1/1 approximant. Such segregation tends to fix the movement of the inner tetrahedron. The problem which model, dynamic or static displacement, is correct for Au–Al–Tm is an important subject to be solved in the future.

TABLE Structure model of Au–Al–Tm 1/1 cubic approximant. Occupancy of the site M7 is 16.7%. See [2] for details in Au–Al–Yb system.

Site	Atom	Set	x	y	z	B [Å^2]	Au–Al–Yb
M1	0.683 Au + 0.317 Al	48h	0.3413(1)	0.1965(2)	0.1090(1)	1.01(4)	0.728 Au + 0.272 Al
M2	0.396 Au + 0.604 Al	24g	0	0.2478(4)	0.0870(3)	2.4(1)	0.380 Au + 0.620 Al
M3	0.914 Au + 0.086 Al	24g	0	0.5972(2)	0.6507(2)	0.93(5)	0.882 Au + 0.118 Al
M4	0.850 Au + 0.150 Al	16f	0.1529(1)	–	–	1.40(7)	0.956 Au + 0.044 Al
M5	0.035 Au + 0.965 Al	12e	0.191(1)	0	1/2	0.6(3)	0.033 Au + 0.967 Al
M6	0.449 Au + 0.551 Al	12d	0.3963(5)	0	0	1.7(2)	0.411 Au + 0.589 Al
M7	0.087 Au + 0.080 Al	48h	0.060(1)	0.029(1)	0.089(1)	4.0(6)	0.078 Au + 0.089 Al
M8	Al	8c	1/4	1/4	1/4	4.5(8)	0.92 Al
Tm	Tm	24g	0	0.1887(2)	0.3038(2)	0.12(5)	Yb

4. Conclusion

In the Au–Al–Tm system, we have observed the icosahedral quasicrystal and the corresponding 1/1 cubic approximant in the narrow composition region. The approximant is an isostructure to the Au–Al–Yb approximant with the replacement of Yb by Tm. These two approximants have very similar atomic arrangements with respect to the Au–Al chemical ordering. From this fact, it is possible to speculate that the corresponding quasicrystals may also have very similar structure. The quasicrystal is an equilibrium phase in the Au–Al–Tm system, and is formed by a peritectic or peritectoid reaction. In order to synthesize large single-domain sample, one needs to think of this situation. The similarity in Au–Al–Yb and Au–Al–Tm quasicrystals as well as in the corresponding approximants may be useful to understand their physical properties, for example, the behavior of non-Fermi liquid recently reported for the Au–Al–Yb quasicrystal and approximant [16, 17].

Acknowledgments

The authors thank N. Miyazaki and S. Yoneda for their help and advice in the use of EPMA, and M. Mihalković for valuable discussion on the state of the inner tetrahedron.

References

[1] J.Q. Guo, E. Abe, A.P. Tsai, *Jpn. J. Appl. Phys.* **39**, L770 (2000).

[2] T. Ishimasa, Y. Tanaka, S. Kashimoto, *Philos. Mag.* **91**, 4218 (2011).

[3] A.P. Tsai, C.P. Gómez, in: *Handbook of Metal Physics: Quasicrystals*, Eds. T. Fujiwara, Y. Ishii, Elsevier, Amsterdam 2008, p. 75.

[4] T. Ishimasa, in Ref. [3], p. 49.

[5] M. Mihalković, C.L. Henley, *Phys. Rev. B* **85**, 092102 (2012).

[6] H. Euchner, T. Yamada, H. Schober, S. Rols, M. Mihalkovic, R. Tamura, T. Ishimasa, M. de Boissieu, *J. Phys., Condens. Matter.* **24**, 415403 (2012).

[7] C.P. Gómez, S. Lidin, *Phys. Rev. B* **68**, 024203 (2003).

[8] Q. Lin, J.D. Corbett, *Inorg. Chem.* **43**, 1912 (2004).

[9] A. Singh, J.Q. Guo, A.P. Tsai, *Mater. Sci. Eng. A* **449/451**, 991 (2007).

[10] Y. Morita, A.P. Tsai, *Jpn. J. Appl. Phys.* **47**, 7975 (2008).

[11] Q. Lin, J.D. Corbett, *Inorg. Chem.* **49**, 4570 (2010).

[12] G.H. Gebresenbut, R. Tamura, D. Eklöf, C.P. Gómez, *J. Phys. Condens. Matter* **25**, 135402 (2013).

[13] S. Kenzari, V. Demange, P. Boulet, M.C. de Weerd, J. Ledieu, J.M. Dubois, V. Fournée, *J. Phys., Condens. Matter* **20**, 095218 (2008).

[14] F. Izumi, T. Ikeda, *Mater. Sci. Forum* **321-324**, 198 (2000).

[15] T.C. Ozawa, S.J. Kang, *J. Appl. Crystallogr.* **37**, 679 (2004).

[16] T. Watanuki, S. Kashimoto, D. Kawana, T. Yamazaki, A. Machida, Y. Tanaka, T.J. Sato, *Phys. Rev. B* **86**, 094201 (2012).

[17] K. Deguchi, S. Matsukawa, N.K. Sato, T. Hattori, K. Ishida, H. Takakura, T. Ishimasa, *Nature Mater.* **11**, 1013 (2012).